LRP1 involvement in FHIT-regulated HER2 signaling in non-small cell lung cancer

Théophile Ponchel, Emma Loeffler, Julien Ancel, Audrey Brisebarre, Nathalie Lalun, Véronique Dalstein, Anne Durlach, Gaëtan Deslée, Stéphane Dedieu, Myriam Polette, et al.

European Journal of Cell Biology 104 (2025) 151475

Contents lists available at ScienceDirect

European Journal of Cell Biology

journal homepage: www.elsevier.com/locate/ejcb

LRP1 involvement in FHIT-regulated HER2 signaling in non-small cell lung cancer

Théophile Ponchel [a], Emma Loeffler [a], Julien Ancel [a,b], Audrey Brisebarre [a], Nathalie Lalun [a], Véronique Dalstein [a,c], Anne Durlach [a,c], Gaëtan Deslée [a,c], Stéphane Dedieu [d], Myriam Polette [a,c], Béatrice Nawrocki-Raby [a,*]

[a] Université de Reims Champagne-Ardenne, INSERM, P3Cell, UMR-S 1250, Reims, France
[b] CHU de Reims, Hôpital Maison Blanche, Service de Pneumologie, Reims, France
[c] CHU de Reims, Pôle de Biologie Territoriale, Service de Pathologie, Reims, France
[d] Université de Reims Champagne-Ardenne, CNRS, MEDyC, UMR 7369, Reims, France

ARTICLE INFO

Keywords:
NSCLC
FHIT
HER2
LRP1
EMT

ABSTRACT

The tumor suppressor fragile histidine triad (FHIT) is frequently lost in non-small cell lung cancer (NSCLC). We previously showed that a down-regulation of FHIT causes an up-regulation of the activity of HER2 associated to an epithelial-mesenchymal transition (EMT) and that lung tumor cells harboring a $FHIT^{low}$/$pHER2^{high}$ phenotype are sensitive to anti-HER2 drugs. Here, we sought to decipher the FHIT-regulated HER2 signaling pathway in NSCLC. Transcriptomic analysis of tumor cells isolated from NSCLC revealed the endocytic receptor low density lipoprotein receptor-related protein 1 (LRP1), a central regulator of membrane trafficking and cell signaling, as a potential player of this signaling. In a cohort of 80 NSCLC assessed by immunohistochemistry, we found a significant association between a low FHIT expression and a high pHER2 and LRP1 expression by tumor cells. Experiments of FHIT silencing showed that FHIT regulated LRP1 expression both at the mRNA and protein levels in lung cell lines. Analyzing the relationship between LRP1 and HER2, we observed that an anti-HER2 targeted therapy reversed LRP1 overexpression induced by FHIT silencing whereas LRP1 silencing did not affect HER2 activity. Studying the functional role of LRP1, we showed that cell proliferation and invasion induced by FHIT silencing were LRP1-dependent. In addition, we found that the induction of vimentin upon FHIT inactivation was counteracted by LRP1 silencing. These results suggest that LRP1 acts downstream of HER2 to induce EMT and tumor progression following FHIT loss. Dual targeting of HER2 and LRP1 might represent a therapeutic strategy to more efficiently inhibit HER2 signaling in FHIT-negative NSCLC.

1. Introduction

Despite a significant improvement of patient outcome thanks to targeted therapy and immunotherapy development in the last two decades, lung cancer, mainly consisting in the non-small cell lung cancer (NSCLC) type, remains a leading cause of cancer-related death worldwide (Sung et al., 2021; Thai et al., 2021). A better knowledge of lung tumor cell biology to find new therapeutic perspectives is therefore a major concern.

Fragile histidine triad (FHIT) is a diadenosine triphosphate (AP3A) hydrolase belonging to the histidine triad (HIT) family (Ohta et al., 1996). FHIT loss is a common event in many cancers including NSCLC (Pekarsky et al., 2002; Sozzi et al., 1996). FHIT is considered as a tumor suppressor notably through its ability to promote genome stability, inhibit cell proliferation and induce apoptosis (Niu et al., 2023; Pekarsky et al., 2002; Roz et al., 2002; Saldivar et al., 2012). Furthermore, we and

Abbreviations: ADC, adenocarcinoma; Ap3A, diadenosine triphosphate; EGFR, epidermal growth factor receptor; EMT, epithelial-mesenchymal transition; FHIT, fragile histidine triad; HIT, histidine triad; LUAD, lung adenocarcinoma; HER2, human epidermal growth factor receptor 2; LDLR, low-density lipoprotein receptor, LRP1, Low-density lipoprotein receptor-related protein 1; NSCLC, non-small cell lung cancer; SCC, squamous cell carcinoma; TKI, tyrosine kinase inhibitor; TNM, tumor node metastasis.

* Correspondence to: Béatrice Nawrocki-Raby, Université de Reims Champagne-Ardenne, INSERM UMR-S 1250, CHU Maison Blanche, 45 rue Cognacq-Jay, REIMS F-51100, France

E-mail address: beatrice.raby@univ-reims.fr (B. Nawrocki-Raby).

https://doi.org/10.1016/j.ejcb.2024.151475
Received 17 May 2024; Received in revised form 13 December 2024; Accepted 26 December 2024
Available online 26 December 2024

others have also reported that FHIT prevents tumor invasion and metastasis by negatively regulating epithelial-mesenchymal transition (EMT), a phenotypic conversion characterized by a progressive decrease of epithelial characteristics and a gain of mesenchymal traits in tumor cells enhancing their aggressiveness (Joannes et al., 2014, 2010; Niu et al., 2023; Suh et al., 2014). More recently, we showed that FHIT regulates the activity of HER2 in lung tumor cells. Indeed, FHIT loss induces an increase of phospho-HER2 (pHER2) level, a sign of HER2 hyperactivation (Da Silva et al., 2020). As a consequence, tumor cells harboring a $FHIT^{low}$/$pHER2^{high}$ phenotype are sensitive to an anti-HER2 therapy. Anti-HER2 drugs restore a more epithelial phenotype, in particular by decreasing the expression of the mesenchymal marker vimentin, and counteract cell invasiveness and growth of FHIT-silenced lung tumor cells (Da Silva et al., 2020). Thus, besides the three well-known molecular alterations of HER2, namely gene mutation, gene amplification and protein overexpression, we described a new type of NSCLC HER2 alteration that is phenotypic and potentially druggable (Loeffler et al., 2023). However, the molecular actors of this FHIT-dependent HER2 signaling pathway remain unknown.

Low-density lipoprotein receptor-related protein 1 (LRP1) is a high molecular weight transmembrane receptor belonging to the low-density lipoprotein receptor (LDLR) family (Herz et al., 1988). As a multifunctional endocytic receptor, LRP1 is distinguished by its ability to bind over fifty different ligands and is known to modulate many cellular processes including lipid homeostasis, cell apoptosis, differentiation, growth and migration (Sizova et al., 2023; Strickland et al., 1990). As LRP1 orchestrates the interplay of membrane trafficking and cell signaling (Van Gool et al., 2015), it emerges as a promising candidate participating in the FHIT-HER2 signaling axis.

Here, we sought to decipher the HER2 signaling pathway upon FHIT loss in lung tumor cells by investigating the functional involvement of LRP1. For that purpose, we analyzed the expression of FHIT, pHER2 and LRP1 in NSCLC samples and used *in vitro* strategies of FHIT and LRP1 silencing as well as HER2 inhibition.

2. Materials and methods

2.1. Study approval

Human study was conducted in accordance with the ethical guideline of the Declaration of Helsinki. Human tumors were obtained from the Tumor Bank of the Reims University Hospital Biological Resource Collection No. AC-2019–340 declared at the Ministry of Health according to the French Law, for use of tissue samples for research. Surgically resected tumors were collected after obtaining informed consent from patients with NSCLC. Access to patient data for this non-interventional study was approved by the French national commission CNIL (Comité National de l'Informatique et des Libertés) (No.2049775 v 0).

2.2. Human tumor samples

The paraffin-embedded tumor pieces for immunohistochemistry were obtained from a cohort of 80 patients with NSCLC including 48 adenocarcinomas and 32 squamous cell carcinomas (Supplementary Table S1).

2.3. Cell lines

Human lung cell lines HBE4-E6/E7, A549, BZR, Calu-1, NCI-H441, NCI-H1838, NCI-H2228 and SK-LU-1 were obtained from the American Type Culture Collection (Rockville, MD, USA), HCC78 from the German Collection of Microorganisms and Cell Cultures DSMZ (Braunschweig, Germany). All culture media and reagents were from Gibco (Invitrogen, Carlsbad, CA, USA). Cells used for experiments were tested for absence of *Mycoplasma* by MycoGenie Rapid Mycoplasma Detection Kit (Dublin, Ireland) and passaged for fewer than four months after resuscitation. A549 and BZR were cultured in DMEM containing 10 % fetal calf serum (FCS), NCI-H441, NCI-H1838, NCI-H2228 and HCC78 in RPMI containing 10 % FCS, Calu-1 and SK-LU-1 in MEM containing 10 % FCS and supplemented with 1x MEM non-essential amino acids and 1 mM sodium pyruvate, and HBE4-E6/E7 in Keratinocyte-SFM supplemented with 0.2 ng/ml EGF and 25 μg/ml bovine pituitary extract. A549 KO FHIT and their control were obtained by CRISPR/Cas9 technology as previously described and cultured like parental A549 cells (Da Silva et al., 2020).

2.4. Anti-HER2 drugs

The HER2 tyrosine kinase inhibitor (TKI) tucatinib (HY-16069) and the humanized monoclonal antibody anti-HER2 trastuzumab (HY-P9907) were purchased from MedChemtronica (Sollentuna, Sweden). A 24h-treatment of cells with both drugs was performed as previously described (Da Silva et al., 2020).

2.5. Antibodies

Antibodies used for immunohistochemistry (IHC), proximity ligation assay (PLA), immunofluorescence (IF), western blotting (WB) and immunoprecipitation (IP) were as follows: rabbit polyclonal antibodies to FHIT (WB: 1:500; ab170888, Abcam, Cambridge, UK), total HER2 (WB after IP: 1:500; PLA:1:100; cat n° 06–562, Millipore, Merck KGaA, Darmstadt, Germany), phospho-HER2 (pHER2) (Tyr1248) (IHC: 1:400 and WB: 1:1000; cat n° 06–229, Millipore) and LRP1 β chain (WB: 1:10000; ab92544, Abcam); rabbit monoclonal antibody to FHIT (IHC: 1:3000; cat n° 14434-R104, Sino Biological, Beijing, China) and total EGFR (WB: 1:10000; clone E235, cat n° 04–338, Millipore); goat polyclonal antibody to TGFβRII (WB: 1:100; AF-241-NA, R&D systems, Bio-Techne, Mineapolis, MN); mouse monoclonal antibodies to total HER2 (WB: 1:500; NCL-L-CB11, Leica Biosystems, Newcastle, UK and IP: 2 μg / 500 μg protein extract; Ab5 clone TA-1, cat n° MABE320, Millipore), LRP1 α chain (IHC: 1:150; PLA: 1:1000; IP: 2 μg / 500 μg protein extract; clone 8G1, cat n° 438190, Millipore), vimentin (IF: 1:200; WB: 1:10000, clone V9, Dako, Glostrup, Denmark) and GAPDH (WB: 1:75000; clone 6C5, Chemicon, Millipore, Billerica, MA, USA).

2.6. Immunohistochemistry

Immunohistochemistry for FHIT, pHER2 and LRP1 was done on serial paraffin tissue sections. After antigen retrieval in Target Retrieval Solution, pH9 (Dako) and endogenous peroxidase inhibition in Bloxall Blocking Solution (Vector laboratories, Burlingame, CA), subsequent steps were performed with the ImmPress HRP Reagent kit peroxidase anti-Rabbit IgG or anti-Mouse IgG (Vector laboratories), and HRP activity was revealed with Immpact NovaRed peroxidase substrate kit (Vector laboratories). The extent of staining was graded on a scale of 0 −4 (0, no staining; 1, ≤ 10 %; 2, 11 −25 %; 3, 26 −50 % and 4, > 50 % of positive tumor cells) and the staining intensity was graded on a scale of 0 −3 (0, no staining; 1, low; 2, medium; 3, high). The extent score was multiplied by the intensity score to obtain the immunostaining score (0 −12). A cut-off at the median score was used to discriminate between low and high expression of each protein.

2.7. Transfection of FHIT and LRP1 small interfering RNA

Cells were transfected with a mix of three siRNA duplexes (20 nM) by calcium phosphate-precipitation method. The sequences were as follow: FHIT si1 5'-CAUCUCAUCAAGCCCUCUG-3', FHIT si2 5'-GGAAGGCUGGAGACUUUCA-3' and FHIT si3 5'-GGAGGACUUUCCUGCCUCU-3'; LRP1 si1 5'-GCUCGUCGACAGCAAGAUU-3', LRP1 si2 5'-GACGAGGAACCGUUUCUGA-3' and LRP1 si3 5'-GCCCUUCCGUUGCAAGAAU-3' (Eurogentec, Seraing, Belgium). Three corresponding scrambled

duplexes which do not recognize any sequence in the human genome were used as controls.

2.8. Western blotting

Protein extracts were obtained by cell lysis in RIPA buffer containing proteases and phosphatases inhibitors. Western blot analyses were done with Mini-Protean TGX 4–20 % precast gels (Bio-Rad Laboratories, Hercules, CA) and the Trans-Blot Turbo Transfer system (Bio-Rad). Detection steps were performed with HRP-conjugated secondary anti-mouse or anti-rabbit antibody (Dako, Glostrup, Denmark) and Amersham ECL Prime kit (GE Healthcare, Little Chalfont, Buckinghamshire, UK). Chemiluminescent signals were acquired with the LAS-4000 imager (Fujifilm, Minato-Ku, Tokyo, Japan).

2.9. RT-qPCR

Total RNA was isolated using the High Pure RNA isolation kit (Roche Diagnostics GmbH, Mannheim, Germany). Total RNA was reverse-transcribed into cDNA with the Transcriptor First Strand cDNA Synthesis kit (Roche Diagnostics). qPCR reactions were performed using the "Fast Start Universal Probe Master" kit and the UPL-probe system as recommended by the manufacturer (Roche Diagnostics), in a Light-Cycler 480 Instrument (Roche Diagnostics). Forward and reverse primers (Eurogentec) for LRP1 and GAPDH were as follow: LRP1 forward 5'-TCAACAACGGTGACTGCTCC-3' and LRP1 reverse 5'-GGAGAAAGGAACCTACGCCC-3'; GAPDH forward 5'-ACCAGGTGGTCTCCTCTGAC-3' and GAPDH reverse 5'- TGCTGTAGCCAAATTCGTTG-3'.

2.10. Proximity ligation assay

Cells cultured on glass coverslips were fixed with 4 % paraformaldehyde, permeabilized with 0.1 % Triton X-100 before analysis of HER2/LRP1 interaction with the Duolink In Situ Red Starter Kit Mouse/Rabbit according to the manufacturer's instructions (Sigma-Aldrich, St Louis, MO). Negative controls were obtained by omitting one or both primary antibodies. PLA signals were quantified using ImageJ software (http://imageJ.nih.gov/ij/index.html).

2.11. Immunoprecipitation

Protein extracts were obtained by cell lysis in RIPA buffer containing proteases and phosphatases inhibitors. Five-hundred μg of total proteins were incubated with 2 μg of HER2 or LRP1 antibody. Nonimmune IgGs were used for negative controls. Immunoprecipitation was performed with protein G Sepharose Fast Flow (Sigma, St Louis, MO). After solubilization under reducing conditions protein complexes were subjected to Western blotting.

2.12. MTT assay

Cells were seeded in 12-well plates at a concentration of 30,000 cells per well. The number of viable cells was evaluated by MTT assay 48 h after plating. Briefly, cells were incubated with 1 mg/ml MTT reagent (Sigma-Aldrich, Saint Louis, MO) during 2 h. Cells were then lysed with propan-2-ol and absorbance of each well was measured at 560 nm using a microplate reader. Experiments were performed with three replicates for each group.

2.13. Invasion assay

The *in vitro* invasive properties of cells were assessed using a modified Boyden chamber assay. An aliquot of 10^5 cells in serum-free medium was placed in the upper compartment of the invasion chamber (BD BioCoat Matrigel Invasion Chamber, BD Biosciences, Bedford, MA, USA). The lower compartment was filled with medium containing 10 % FCS. The chambers were incubated for 17–24 h at 37 °C. The filters were then fixed in methanol and stained with hematoxylin. Quantification of the invasion assay was performed by counting the number of cells at the lower surface of the filters (23 fields at 400-fold magnification).

2.14. Cell circularity analysis

Cellular circularity was measured with ImageJ software (http://imagej.nih.gov/ij/index.html) according to the following formula: circularity $= 4\pi(\text{area}/\text{perimeter}^2)$.

2.15. Immunofluorescence

Cells cultured on glass coverslips were fixed with methanol before blocking in a 3 % BSA solution and incubation with vimentin primary antibody followed by Alexa Fluor 594-coupled secondary anti-mouse antibody (Invitrogen, Eugene, OR). Nuclei were counterstained with DAPI. Mean fluorescence intensity per cell was quantified with ImageJ software (http://imagej.nih.gov/ij/index.html).

2.16. RNA databases analysis

Gene expression data for 106 NSCLC cell lines including 79 adenocarcinoma and 27 squamous cell carcinoma cell lines belonging to the Cancer Cell line Encyclopedia (Ghandi et al., 2019) and for 169 lung adenocarcinoma samples of the LUAD OncoSG dataset (Chen et al., 2020) were acquired through cBioPortal (https://portal.gdc.cancer.gov/) (Cerami et al., 2012; de Bruijn et al., 2023; Gao et al., 2013). The mRNA expression profiles were extracted and processed in the log RNA Seq V2 RSEM format. FHIT and LRP1 statuses were considered as low or high, with expression level below or above the median, respectively.

Aiming to create an EMT signature, we combined three existing EMT signatures and compared mesenchymal with epithelial NSCLC cell lines (Byers et al., 2013; Chae et al., 2018; Mak et al., 2016). Sixty-two genes showed significant differences between these groups. We then used these genes to calculate a log2 unweighted EMT score for each group based on mRNA expression counts, reflecting the balance between mesenchymal and epithelial genes (Supplementary Figure S1 and supplementary Table S2). It should be noted that 2 genes, namely LIX1L and EPPK1, belonging respectively to the mesenchymal and epithelial clusters, were not exploitable in the LUAD-OncoSG database. Consequently, the EMT score was reduced to 60 genes for this database. For each cohort, we defined epithelial, intermediate epithelial/mesenchymal and mesenchymal samples based on tertiles.

2.17. Statistics

Two-tailed Spearman and Pearson tests were used to analyze the correlation between two measured variables. Two-sided Fisher's exact test or Chi-square test were used to analyze the association between two or more categorical variables. *In vitro* data expressed as fold induction were analyzed with a two-tailed one-sample Student's *t*-test. Other data were analyzed with a two-tailed Mann Whitney test or a Kruskal-Wallis test with Dunn's post-hoc test. $P < 0.05$ was considered significant. All analyses were performed using Prism version 9.0 software (GraphPad Software, La Jolla, CA) and XLSTAT version 2022.4.1 software (Addinsoft company, Paris, France). Alluvial plots were produced with the ggalluvial extension of ggplot2 R package (http://ggplot2.tidyverse.org).

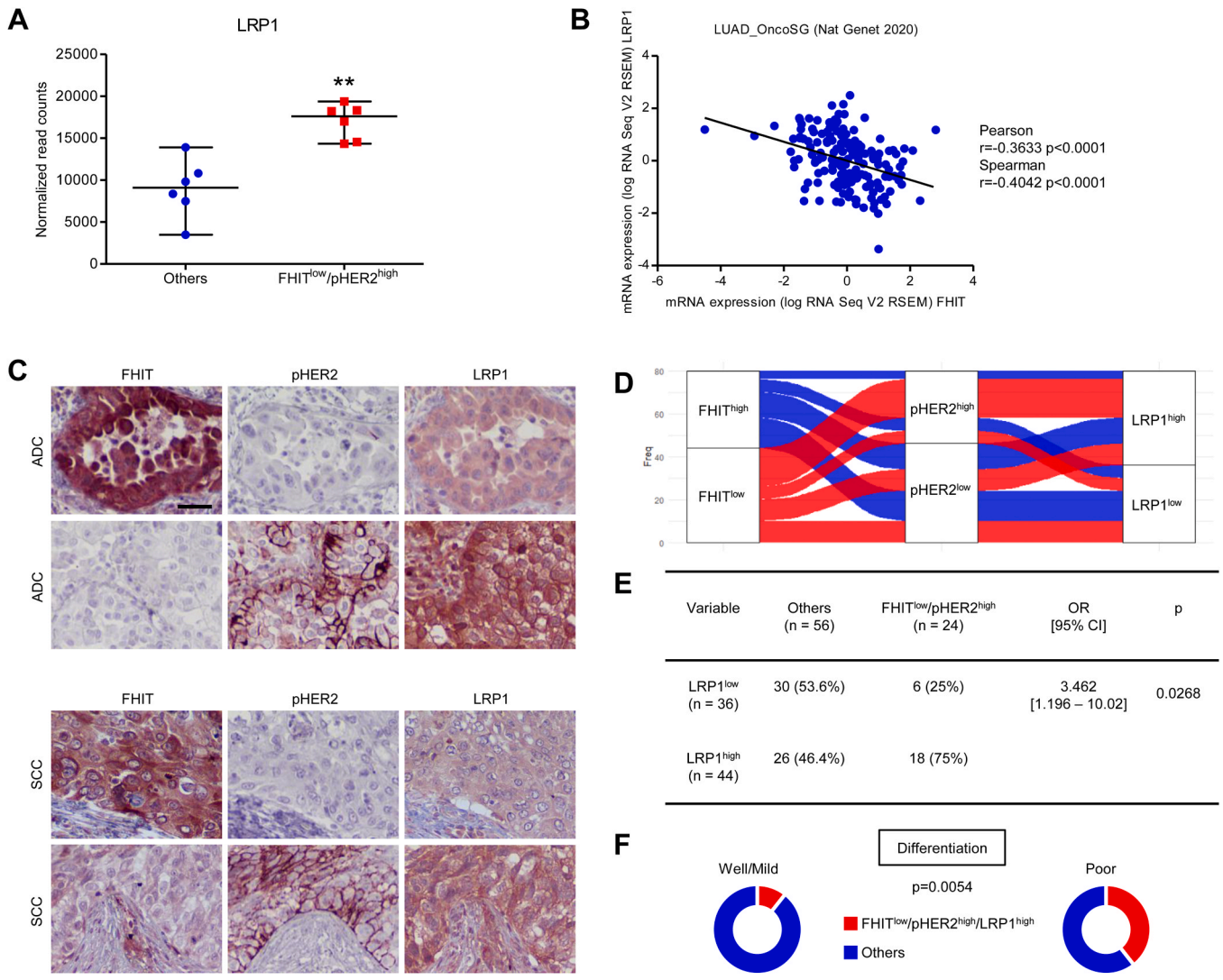

Fig. 1. Association between a high expression of LRP1 and a FHIT^{low}/pHER2^{high} phenotype in NSCLC. **A.** Comparison of LRP1 transcripts levels by Mann-Whitney test between FHIT^{low}/pHER2^{high} tumor cells (red square) and other ones (blue circles) in our transcriptomic dataset of primary tumor cells isolated from NSCLC (GEO accession number GSE208544) (bars and error bars = median with range) (n = 6 per group). * *p < 0.01 **B.** Negative correlation between FHIT and LRP1 mRNA expression in public database of LUAD OncoSG (n = 169). Regression line is represented. **C.** Immunohistochemistry analysis showing FHIT, pHER2 and LRP1 stainings on serial sections of two ADC cases (top) and two SCC cases (bottom) (scale bar = 23 μm). **D.** Alluvial plot showing the relationship between FHIT, pHER2 and LRP1 statuses in the 80 NSCLC. **E.** Fisher' exact test showing association between a high expression of LRP1 and a FHIT^{low}/pHER2^{high} phenotype in the entire series of NSCLC (n = 80). **F.** Distribution of the differentiation status of FHIT^{low}/pHER2^{high}/LRP1^{high} (in red) and other tumors (in blue) in the series of 80 NSCLC (Fisher's exact p-value). Abbreviations: pHER2, phospho-HER2; LUAD, lung adenocarcinoma; ADC, adenocarcinoma; SCC, squamous cell carcinoma.

3. Results

3.1. LRP1 high expression is correlated to a FHIT^{low}/pHER2^{high} phenotype

First, searching for potential players of the FHIT-HER2 signaling axis, we examined our previously published RNA-seq dataset (GEO accession number GSE208544) comparing differentially expressed transcripts between primary tumor cells isolated from NSCLC with a FHIT^{low}/pHER2^{high} phenotype and those displaying other phenotypes (Brisebarre et al., 2022). As a central regulator of membrane trafficking and cell signaling, LRP1 caught our particular attention. LRP1 expression appears either positively or negatively correlated with tumor aggressiveness and prognosis, depending on the tumor type, with limited data available for lung cancer (Boulagnon-Rombi et al., 2018; Feng et al., 2018). In our study, LRP1 mRNA was significantly upregulated in FHIT^{low}/pHER2^{high} tumor cells (17611 versus 9088 normalized read counts, p = 0.022) (Fig. 1A). These data were reinforced by the observation of a negative correlation between FHIT and LRP1 transcripts in the OncoSG lung adenocarcinomas (LUAD) dataset selected from cBioportal (Fig. 1B).

Then, to further investigate the relationship between LRP1, FHIT and pHER2, we analyzed their expression by immunohistochemistry in a cohort of 80 human NSCLC samples including 42 adenocarcinomas (ADC) and 38 squamous cell carcinomas (SCC) (Fig. 1C, Supplementary Table S1). We focused on LRP1, FHIT and pHER2 detection in tumor cells. LRP1 was detected in tumor cells of 79 out of 80 NSCLC samples. It was predominantly localized in the cytoplasm and, to a lesser extent, at the cell membrane. We observed a significant association between a high expression of LRP1, a low expression of FHIT and a high activation of HER2 (Fig. 1D, Supplementary Figure S2A). Seventy-five percent of FHIT^{low}/pHER2^{high} tumors were LRP1^{high} against only 46.4 % of other tumors (Fig. 1E). While LRP1^{high} tumors were not significantly categorized as pHER2^{high} regardless of FHIT expression (Supplementary Figure S2B), pHER2^{high}/LRP1^{high} tumors were significantly associated with a FHIT^{low} status (82 % vs 45 % for other tumors) (Supplementary

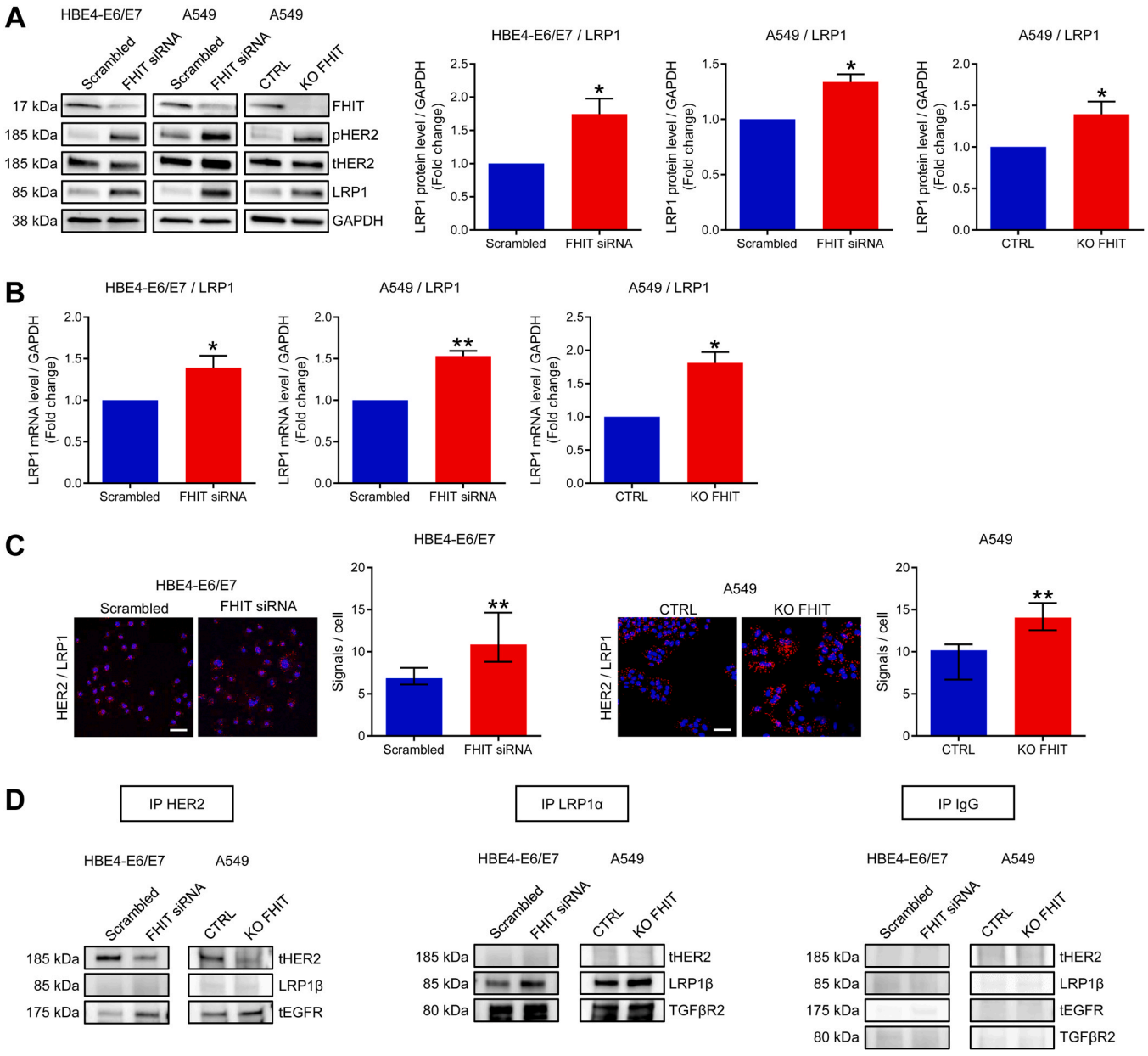

Fig. 2. Regulation of LRP1 expression by FHIT. A. Left, Western blot analysis of FHIT, pHER2, tHER2 and LRP1 levels in HBE4-E6/E7 and A549 cell lines transiently transfected by FHIT siRNA or the scrambled control, and in A549 cell line stably transfected by CRISPR/Cas9 KO FHIT plasmid or the control plasmid. GAPDH served as loading control. Right, Quantification graphs: values represent means and SD (n = 3). One sample *t*-test: *p < 0.05. **B.** RT-qPCR analysis of LRP1 mRNA level in HBE4-E6/E7 and A549 cell lines transiently transfected by FHIT siRNA (red) or the scrambled control (blue) and in A549 cell line stably transfected by CRISPR/Cas9 KO FHIT plasmid (red) or the control plasmid (blue). Values represent means and SD (n = 3). One sample *t*-test: *p < 0.05; * *p < 0.01. **C.** Analysis by the proximity ligation assay of the link between HER2 and LRP1 in HBE4-E6/E7 and A549 cells silenced or not for FHIT by siRNA or by CRISPR/Cas9 (scale bar = 57 μm). Quantification of the number of interactions (red dots) per cell. Nuclei were counterstained with DAPI (blue). (n = 5). Values represent medians and IQR. Two-tailed Mann-Whitney test: * *p < 0.01. **D.** Immunoprecipitation analysis using anti-HER2 and anti-LRP1 α antibodies in HBE4-E6/E7 and A549 cells silenced or not for FHIT by siRNA or by CRISPR/Cas9. Non-immune IgG served as negative control. tEGFR and TGFβRII detection served as positive control for respectively HER2 IP and LRP1α IP. Abbreviations: pHER2, phospho-HER2; tHER2, total HER2; tEGFR, total EGFR, IP, immunoprecipitation.

Figure S2C). These data highlight a filiation between FHIT loss and the correlation between a high LRP1 expression and a HER2 hyper-activation. Interestingly, $FHIT^{low}$/$pHER2^{high}$/$LRP1^{high}$ tumors were more frequently associated with a poor differentiation degree (OR = 5.460; p = 0.0054) (Fig. 1F). No association between the $FHIT^{low}$/$pHER2^{high}$/$LRP1^{high}$ pattern and any other clinical parameters were found.

3.2. LRP1 expression is regulated by FHIT

To study the functional link between LRP1, FHIT and HER2, we used strategies of FHIT transient silencing or knockout in HBE4-E6/E7 and A549 lung cell lines in order to mimic FHIT loss. By Western blot analysis, we showed that transient FHIT silencing in HBE4-E6/E7 cells and transient FHIT silencing or FHIT knockout in A549 cells induced a significant increase of LRP1 level correlated with an increase of HER2 activity (Fig. 2A). This LRP1 increase was confirmed by RT-qPCR (Fig. 2B), thus demonstrating that FHIT regulated LRP1 expression

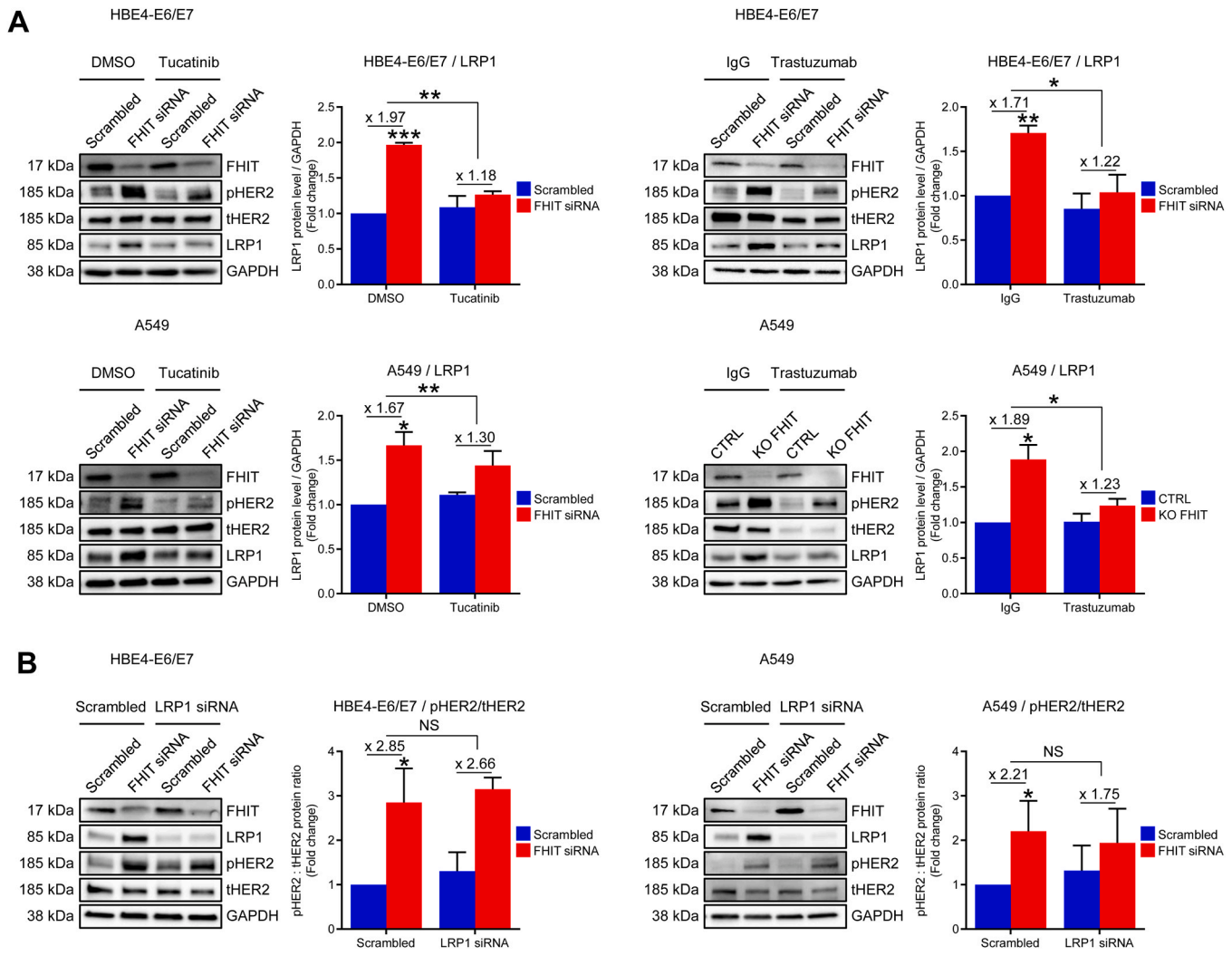

Fig. 3. Involvement of HER2 in LRP1 regulation by FHIT. **A.** Western blot analysis of LRP1 levels in HBE4-E6/E7 (top) and A549 (bottom) knockdown or not for FHIT and treated or not with the anti-HER2 inhibitors tucatinib (10 nM) (left) or trastuzumab (2 μg/ml) (right) during 24 h. GAPDH serves as a loading control. Quantification graphs: values represent means and SD (n = 3); One sample *t*-test: *p < 0.05; * *p < 0.01; * **p < 0.001. **B.** Western blot analysis of HER2 activation rate (pHER2/tHER2) in HBE4-E6/E7 (left) and A549 (right) transiently co-invalidated or not for FHIT and LRP1. GAPDH serves as a loading control. Quantification graphs: values represent means and SD (n = 4); One sample *t*-test: *p < 0.05. Abbreviations: pHER2, phospho-HER2; tHER2, total HER2; NS, non-significant.

both at the mRNA and protein levels concomitantly with HER2 activation in lung cell lines. Considering that LRP1 interacts with a wide range of cell surface receptors, either directly or via molecular complexes, including growth factor receptors, and that previous data demonstrated that EGFR could be recruited to LRP1-rich regions (Cruz Da Silva et al., 2021), we proposed to investigate the spatial proximity of LRP1 and HER2 by proximity ligation assay (PLA) in our tumor context. Interestingly, results presented in Fig. 2C showed a closed proximity between both receptors that was significantly enhanced by FHIT silencing in HBE4-E6/E7 and A549 cells. However, immunoprecipitation experiments failed to observe co-immunoprecipitation between LRP1 and HER2 in HBE4-E6/E7 and A549 cells (Fig. 2D). This observation could imply either a transient interaction or one occurring within a complex molecular network.

3.3. LRP1 acts downstream of HER2 upon FHIT loss

Subsequently, to elucidate the association between LRP1 and HER2 in FHIT-downregulated cells, we explored their reciprocal influence. The influence of HER2 on LRP1 was studied using two anti-HER2 drugs, the TKI tucatinib and the humanized monoclonal antibody trastuzumab. We observed by Western blotting that tucatinib was able to reverse LRP1 overexpression induced by FHIT silencing by 41.22 % (p = 0.008) and 22.16 % (p = 0.005) in HBE4-E6/E7 and A549 cells, respectively. Trastuzumab exhibited a similar effect than tucatinib (reduction of 28.46 % and 34.87 % in HBE4-E6/E7 and A549 cells, respectively; p = 0.011 and p = 0.030) (Fig. 3A).

On the other hand, the influence of LRP1 on HER2 was investigated using LRP1 siRNA. We found that LRP1 silencing did not affect HER2 activity. Indeed, as shown by Western blot analysis, the increase of HER2 activation rate induced by FHIT knockdown was not reduced neither in HBE4-E6/E7 cells nor in A549 cells transfected by LRP1 siRNA transfection (Fig. 3B).

Taken together, these data suggest that LRP1 acts downstream of HER2 in the signaling regulated by FHIT.

3.4. LRP1 is involved in tumor aggressiveness induced by FHIT loss

We therefore studied the functional involvement of LRP1 in the aggressiveness of lung tumor cells induced by the FHIT-HER2 signaling axis. More specifically, we explored the role of LRP1 in cell proliferation and cell invasion, two processes known to be influenced by LRP1 in different tumor contexts (Langlois et al., 2010; Le et al., 2020), and controlled by FHIT and involving HER2 in NSCLC (Da Silva et al., 2020).

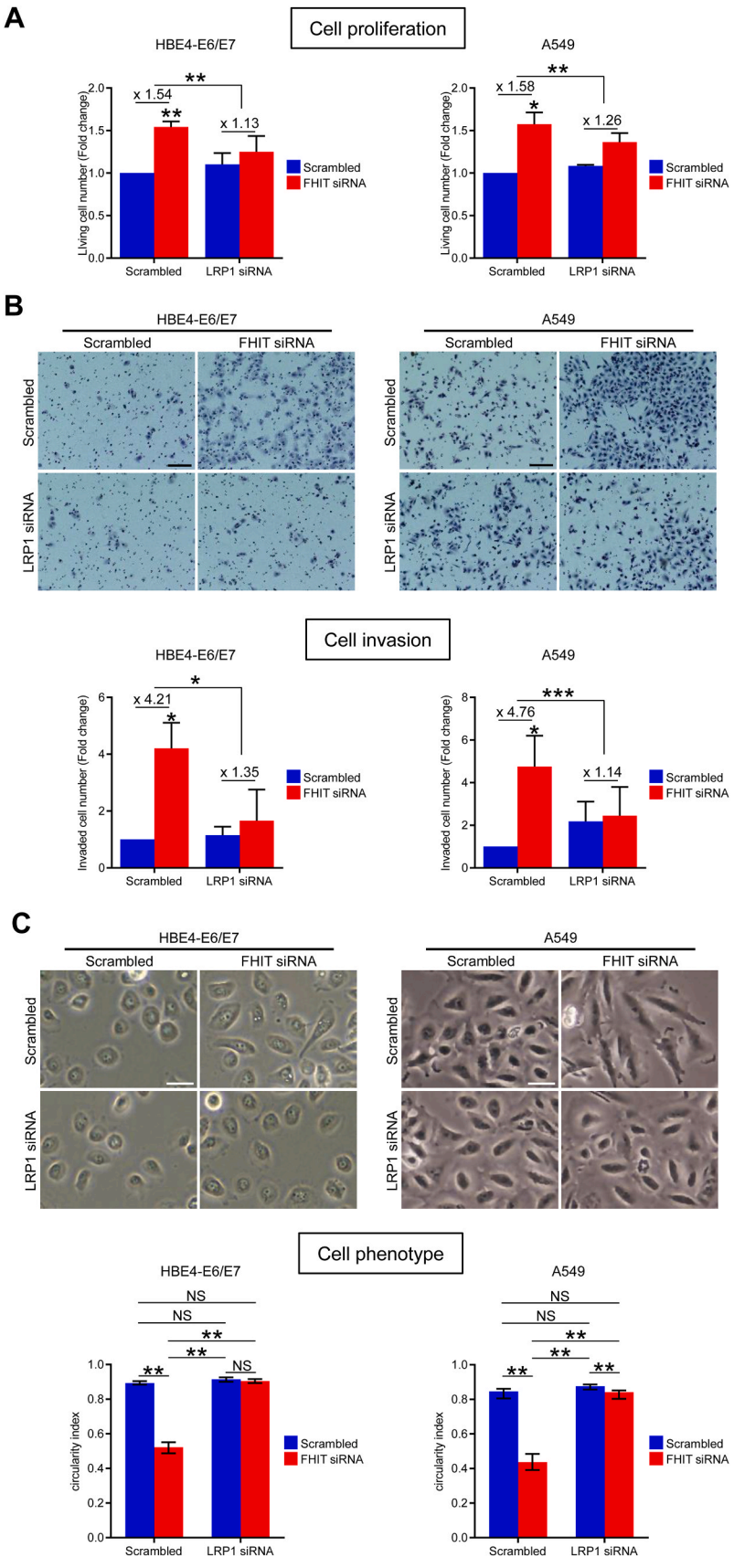

(caption on next page)

Fig. 4. LRP1-dependent cell proliferation and invasion induced by FHIT loss. **A.** Cell proliferation analysis by MTT assay of HBE4-E6/E7 (left) and A549 (right) transiently co-silenced or not for FHIT and LRP1. Quantification graphs: values represent means and SD (n = 3); One sample *t*-test: *p < 0.05; * *p < 0.01. **B.** Analysis of cell invasion capacities in a matrigel modified Boyden chamber assay of HBE4-E6/E7 (left) and A549 (right) transiently co-silenced or not for FHIT and LRP1. Top, representative fields of invading cells (scale bar = 65 μm). Bottom, quantification graphs: values represent means and SD (n = 3); One sample *t*-test: *p < 0.05; * **p < 0.001. **C.** Top, Representative phase-contrast images of cell morphology of HBE4-E6/E7 (left) and A549 (right) transiently co-silenced or not for FHIT and LRP1 (scale bar = 10 μm). Bottom, Measurement of cell circularity index (n = 6). Values represent medians and IQR. Two-tailed Mann-Whitney test: * *p < 0.01. Abbreviation: NS, non-significant.

Cell proliferation analysis assay was performed on HBE4-E6/E7 and A549 cells transiently co-transfected by FHIT and LRP1 siRNA, along with their respective controls. We observed that LRP1 silencing specifically inhibited cell proliferation of FHIT knockdown cells whereas it had no significant effect on control cells. The increase of cell proliferation induced by FHIT siRNA was reduced respectively by 26.73 % and 20.23 % in the presence of LRP1 siRNA in HBE4-E6/E7 and A549 cells ($p = 0.002$ and $p = 0.004$, respectively) (Fig. 4A).

Using Boyden assay, we found that cell invasion induced by FHIT silencing was LRP1-dependent. Indeed, the invasive capacities of HBE4-E6/E7 and A549 transfected by FHIT siRNA were respectively decreased by 67.79 % ($p = 0.011$) and 76.03 % ($p < 0.001$) using LRP1 siRNA (Fig. 4B).

As LRP1 is involved in FHIT-dependent cell invasion, we examined the phenotype of HBE4-E6/E7 and A549 cells after FHIT/LRP1 co-silencing. We observed that FHIT-silenced HBE4-E6/E7 and A549 cells exhibited a more elongated morphology and greater dispersal compared to FHIT-positive control cells. In contrast, cells with co-silencing of FHIT and LRP1 displayed a more rounded morphology and increased cohesion, resembling control cells (Fig. 4C, top). Accordingly, the decrease of circularity index induced by FHIT silencing was reversed by LRP1 co-silencing in both HBE4-E6/E7 and A549 cell lines ($p = 0.0022$ and $p = 0.0022$, respectively) (Fig. 4C, bottom). Therefore, LRP1 silencing might restore a more epithelial phenotype in cells subjected to FHIT loss.

Altogether, these results suggest that LRP1 silencing replicates the previously described effect of HER2 inhibition on the behavior of FHIT-downregulated lung tumor cells.

3.5. *LRP1 is involved in acquisition of EMT in FHIT-downregulated tumor cells*

Following the above data, we investigated the role of LRP1 in EMT regulation. We focused on vimentin, a well-known mesenchymal marker. Western blot analysis allowed to demonstrate that the increase of vimentin level induced by FHIT silencing was counteracted by LRP1 siRNA in both HBE4-E6/E7 and A549 cells (decrease of 27.46 % and 40.42 %, respectively; $p = 0.010$ and $p = 0.042$) (Fig. 5A). Similar results were obtained by immunofluorescence analysis (Fig. 5B). Moreover, through Western blotting analysis conducted on a series of 9 lung tumor cell lines, we noted a negative correlation between FHIT levels and those of LRP1 and vimentin. Conversely, a positive correlation was observed between LRP1 and vimentin levels (Fig. 5C and D). These correlations were corroborated in a transcriptomic dataset from a larger collection of NSCLC cell lines selected from cBioportal (Fig. 5E). As vimentin expression by tumor cells is a hallmark of EMT, we explored the association between FHIT/LRP1 status and a transcriptomic signature of EMT. In the same transcriptomic dataset of NSCLC cell lines, we globally observed that the EMT score significantly varied with the level of FHIT and LRP1 ($p = 0.0075$). Subgroup analysis highlighted that $FHIT^{low}/LRP1^{high}$ cell lines exhibited a significantly higher EMT score than $FHIT^{high}/LRP1^{low}$ ones ($p = 0.001$) (Fig. 5F, left). Distribution analysis of epithelial, epithelial/mesenchymal and mesenchymal phenotypes showed significant differences with the highest proportion of mesenchymal phenotype and the lowest proportion of epithelial phenotype in $FHIT^{low}/LRP1^{high}$ cell lines compared to other ones ($p = 0.0016$) (Fig. 5F, right). Results were even clearer in the LUAD OncoSG dataset. A significant global association between EMT score and FHIT/LRP1 status was observed in adenocarcinomas ($p < 0.0001$). Comparing subgroups, $FHIT^{low}/LRP1^{high}$ adenocarcinomas had a significantly higher EMT score than $FHIT^{high}/LRP1^{high}$ ($p = 0.044$), $FHIT^{low}/LRP1^{low}$ ($p < 0.0001$) and $FHIT^{high}/LRP1^{low}$ ones ($p < 0.0001$) (Fig. 5G, left). The lowest proportion of epithelial phenotype and the highest proportion of mesenchymal phenotype were found in $FHIT^{low}/LRP1^{high}$ adenocarcinomas ($p < 0.0001$) (Fig. 5G, right).

These results highlight that FHIT-mediated regulation of EMT in lung tumor cells is intricately linked to LRP1.

4. Discussion

This study demonstrates that LRP1 acts downstream of HER2 to induce EMT and tumor progression following FHIT loss in lung tumor cells.

First, we observed that a high expression of LRP1 by tumor cells was associated with a low FHIT expression and a high activity of HER2 in NSCLC patients. To date, the role of LRP1 in cancer remains ambiguous. It is sometimes described as providing anti-tumor effect, while in other cases it is a pro-tumor effect, depending strongly on the tissue origin and cell origin. Indeed, a low expression of LRP1 was related to high grade tumors and poor survival in hepatocellular carcinoma, melanoma or colon carcinoma (Boulagnon-Rombi et al., 2018; de Vries et al., 1996; Huang et al., 2012). On the contrary, a higher expression of LRP1 was reported in advanced stages of endometrial, breast or renal cancers (Catasús et al., 2011a,b; Feng et al., 2018). Here, the relationship between a high level of LRP1 and the $FHIT^{low}/pHER2^{high}$ phenotype previously described as predictive of a late stage and a poor outcome in NSCLC thus suggests a role of LRP1 in promoting tumor progression of lung cancer (Brisebarre et al., 2022). Even though little is known about LRP1 in lung, Meng *et al.* were interested in its expression in the tumor microenvironment and reported a lower level of LRP1 mRNA in fibroblasts of lung tumors relative to those of non-tumoral lung tissue (Meng et al., 2011). This highlights a complex regulation of LRP1 expression in the different cell populations of lung tumor.

Then, we showed that FHIT regulates LRP1 expression in a HER2-dependent manner. A link between LRP1 and ErbB family, especially with EGFR, was previously reported. It was demonstrated that LRP1 contributes to gefitinib-mediated EGFR endocytosis in glioma cells (Cruz Da Silva et al., 2021). It was also shown that LRP1 stabilizes activated EGFR at cell surface to sustain breast cancer cell motility in ischemic conditions (Chang et al., 2022). These studies highlight the role of LRP1 in endocytosis/membrane trafficking to regulate EGFR signaling. Our own results are instead in favor of a signaling function for LRP1 under the control of HER2 in conditions of FHIT loss. This hypothesis is also supported by our data showing that, although in close proximity, LRP1 and HER2 did not co-immunoprecipitate in the context of FHIT silencing.

We also provided evidence of LRP1 involvement, at least in part, in cell proliferation and, more obviously, in cell invasion induced by FHIT knockdown. In accordance with these results, it was shown that breast cancer cell growth is facilitated by a mechanism involving LRP1 under hypoxic conditions (Dong et al., 2016). Le *et al.* demonstrated that LRP1 promotes colon cancer cell proliferation in 3D collagen matrices through a DDR1-dependent mechanism (Le et al., 2020). Salama *et al.* also showed that LRP1 controls melanoma growth (Salama et al., 2019). On the other hand, it was described that LRP1 supports breast cancer cell migration, invasion and metastasis development (Berquand et al., 2019; Fayard et al., 2009; Sahu et al., 2012). The role of LRP1 in promoting

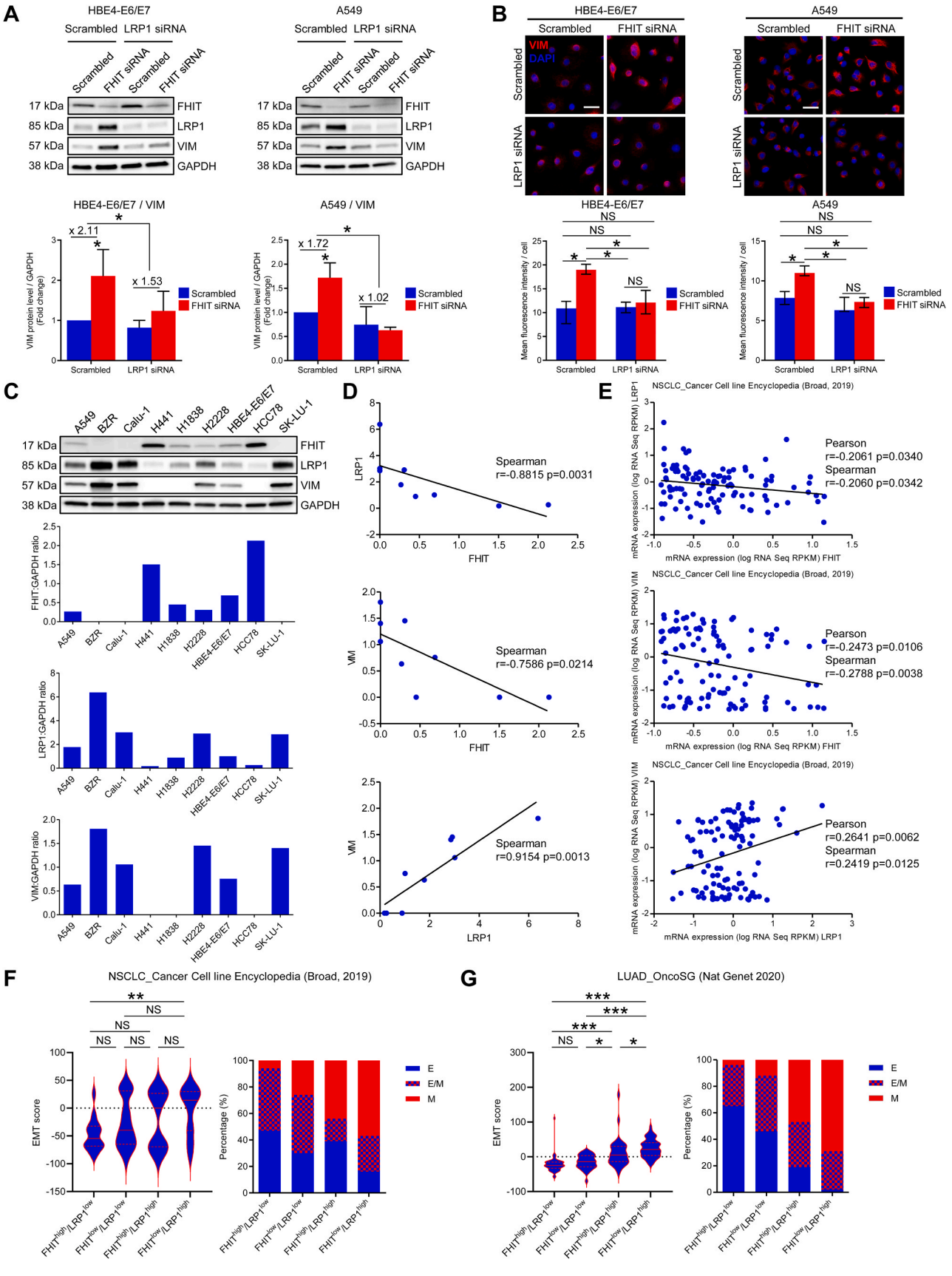

(caption on next page)

Fig. 5. LRP1-dependent EMT induced by FHIT loss. **A.** Western blot analysis of vimentin in HBE4-E6/E7 (left) and A549 (right) transiently co-silenced or not for FHIT and LRP1. GAPDH served as loading control. Quantification graphs: values represent means and SD (n = 4); One sample *t*-test: *p < 0.05. **B.** Top, Immunofluorescence detection of vimentin (red) in HBE4-E6/E7 (left) and A549 (right) transiently co-silenced or not for FHIT and LRP1. Nuclei were counterstained with DAPI (blue). (scale bar = 28 μm). Bottom, Quantification of mean fluorescence intensity per cell (n = 4). Values represent medians and IQR. Two-tailed Mann-Whitney test: *p < 0.05. **C.** Western blot analysis of FHIT, LRP1 and vimentin in a series of 9 lung tumor cell lines. Top, Blots of cell lines. Levels of GAPDH served as loading controls. Bottom, Quantification graphs. **D.** Negative correlation between FHIT level and LRP1 and vimentin levels and positive correlation between LRP1 and vimentin levels in the 9 lung tumor cell lines. Regression lines are represented. **E.** Negative correlation between FHIT level and LRP1 and vimentin levels and positive correlation between LRP1 and vimentin levels in the NSCLC cell lines (n = 106) selected from the transcriptomic dataset of Cancer Cell line Encyclopedia provided by cBioportal. Regression lines are represented. **F.** Left, Comparison of EMT scores according to the FHIT/LRP1 status in NSCLC cell lines from the public transcriptomic dataset of Cancer Cell line Encyclopedia (n = 106) (bars and error bars = median with range). Dunn's post-hoc test: * *p < 0.01. Right, Distribution of epithelial (E, blue), epithelial/mesenchymal (E/M, cross-hatched blue and red) and mesenchymal (M, red) phenotypes according to FHIT/LRP1 status in the same cell lines. **G.** Left, Comparison of EMT scores according to the FHIT/LRP1 status in adenocarcinomas from the public LUAD OncoSG transcriptomic dataset (n = 169) (bars and error bars = median with range). Dunn's post-hoc test: *p < 0.05; * **p < 0.001. Right, Distribution of epithelial (E, blue), epithelial/mesenchymal (E/M, cross-hatched blue and red) and mesenchymal (M, blue) phenotypes according to the FHIT/LRP1 status in the same cohort Abbreviations: VIM, vimentin; NS, non-significant.

tumor cell motility was also reported in other cancer cell types such as glioblastoma, thyroid cancer, pancreatic cancer and melanoma (Langlois et al., 2010; Salama et al., 2019; Song et al., 2009; Xue et al., 2022).

Finally, we showed that regulation of EMT, especially vimentin, by FHIT engages LRP1. This result is strengthened by our finding on the association of $FHIT^{low}$/$pHER2^{high}$/$LRP1^{high}$ profile with a poor differentiation of NSCLC and also our observation of a link between EMT and FHIT/LRP1 status in public datasets of NSCLC cell lines and LUAD. Consistent with these data, LRP1 was demonstrated to sustain tumor cell aggressiveness through its ability to induce EMT in cooperation with eHSP90α in pancreatic and breast cancers (Tian et al., 2019; Xue et al., 2022).

While our data establishes a clear functional link between LRP1 and HER2, the underlying molecular mechanism remains unclear. The ability of LRP1 to integrate deleterious signals from the tumor microenvironment to drive signaling processes, must be considered. It is conceivable that LRP1 may cooperate with HER2 by modulating the trafficking or signaling of downstream effectors such as PI3K/AKT, ERK1/2, or STAT3, which are established mediators of proliferation and survival in NSCLC cells. Furthermore, LRP1 is reported to regulate cytoskeletal dynamics and adhesion molecules and was involved in promoting mesenchymal markers such as Snail and vimentin, hallmarks of EMT (Xue et al., 2022). It is also conceivable that LRP1 may promote EMT by stabilizing HER2-induced signaling complexes responsible for a mesenchymal phenotype. Future investigations should focus on identifying specific intermediates downstream of LRP1 that mediate its effects on proliferation, invasion, and EMT.

In conclusion, our data highlight a new role for LRP1 in tumor progression of NSCLC and bring new insights into the FHIT-HER2 signaling axis. Dual targeting of HER2 and LRP1 might represent a therapeutic strategy to more efficiently inhibit HER2 signaling in FHIT-negative NSCLC.

Funding

This work was supported by grants from La Ligue Contre le Cancer (Committees of Ardennes, Doubs-Montbéliard, Marne, and Meuse) and Lions Club of Soissons, Villers-Cotterets and Crépy-en-Valois. T.P. was supported by the University of Reims Champagne-Ardenne. E.L. was supported by the Région Grand Est and INSERM. J.A. was supported by ITMO Cancer of Aviesan.

CRediT authorship contribution statement

Béatrice Nawrocki-Raby: Writing – review & editing, Writing – original draft, Visualization, Validation, Supervision, Project administration, Methodology, Investigation, Funding acquisition, Formal analysis, Conceptualization. **Myriam Polette:** Writing – review & editing, Resources, Project administration, Funding acquisition. **Emma Loeffler:** Writing – review & editing, Investigation. **Théophile Ponchel:** Writing – review & editing, Validation, Methodology, Investigation, Formal analysis. **Anne Durlach:** Writing – review & editing, Resources. **Véronique Dalstein:** Writing – review & editing, Resources. **Stéphane Dedieu:** Writing – review & editing. **Gaëtan Deslée:** Writing – review & editing, Resources. **Nathalie Lalun:** Writing – review & editing, Investigation. **Audrey Brisebarre:** Writing – review & editing, Formal analysis, Data curation. **Julien Ancel:** Writing – review & editing, Resources, Formal analysis, Data curation.

Declaration of Competing Interest

The authors declare that they have no known competing financial interests or personal relationships that could have appeared to influence the work reported in this paper.

Acknowledgments

The results shown here are in part based upon data generated by the Broad Cancer Cell Line Encyclopedia: https://depmap.org/portal/download/all/?releasename=CCLE+ 2019 and the OncoSG Lung Cancer Consortium Singapore: https://src.gisapps.org/OncoSG/.

Appendix A. Supporting information

Supplementary data associated with this article can be found in the online version at doi:10.1016/j.ejcb.2024.151475.

References

Berquand, A., Meunier, M., Thevenard-Devy, J., Ivaldi, C., Campion, O., Dedieu, S., Molinari, M., Devy, J., 2019. A gentle approach to investigate the influence of LRP-1 silencing on the migratory behavior of breast cancer cells by atomic force microscopy and dynamic cell studies. Nanomed. Nanotechnol. Biol. Med. 18, 359–370. https://doi.org/10.1016/j.nano.2018.10.012.

Boulagnon-Rombi, C., Schneider, C., Leandri, C., Jeanne, A., Grybek, V., Bressenot, A.M., Barbe, C., Marquet, B., Nasri, S., Coquelet, C., Fichel, C., Bouland, N., Bonnomet, A., Kianmanesh, R., Lebre, A.-S., Bouché, O., Diebold, M.-D., Bellon, G., Dedieu, S., 2018. LRP1 expression in colon cancer predicts clinical outcome. Oncotarget 9, 8849–8869. https://doi.org/10.18632/oncotarget.24225.

Brisebarre, A., Ancel, J., Ponchel, T., Loeffler, E., Germain, A., Dalstein, V., Dormoy, V., Durlach, A., Delepine, G., Deslée, G., Polette, M., Nawrocki-Raby, B., 2022. Transcriptomic FHITlow/pHER2high signature as a predictive factor of outcome and immunotherapy response in non-small cell lung cancer. Front. Immunol. 13, 1058531. https://doi.org/10.3389/fimmu.2022.1058531.

de Bruijn, I., Kundra, R., Mastrogiacomo, B., Tran, T.N., Sikina, L., Mazor, T., Li, X., Ochoa, A., Zhao, G., Lai, B., Abeshouse, A., Baiceanu, D., Ciftci, E., Dogrusoz, U., Dufilie, A., Erkoc, Z., Garcia Lara, E., Fu, Z., Gross, B., Haynes, C., Heath, A., Higgins, D., Jagannathan, P., Kalletla, K., Kumari, P., Lindsay, J., Lisman, A., Leenknegt, B., Lukasse, P., Madela, D., Madupuri, R., van Nierop, P., Plantalech, O., Quach, J., Resnick, A.C., Rodenburg, S.Y.A., Satravada, B.A., Schaeffer, F., Sheridan, R., Singh, J., Sirohi, R., Sumer, S.O., van Hagen, S., Wang, A., Wilson, M., Zhang, H., Zhu, K., Rusk, N., Brown, S., Lavery, J.A., Panageas, K.S., Rudolph, J.E., LeNoue-Newton, M.L., Warner, J.L., Guo, X., Hunter-Zinck, H., Yu, T.V., Pilai, S., Nichols, C., Gardos, S.M., Philip, J., AACR Project GENIE BPC Core Team, AACR Project GENIE Consortium, Kehl, K.L., Riely, G.J., Schrag, D., Lee, J., Fiandalo, M.V., Sweeney, S.M., Pugh, T.J., Sander, C., Cerami, E., Gao, J., Schultz, N., 2023. Analysis

and visualization of longitudinal genomic and clinical data from the AACR Project GENIE biopharma collaborative in cBioPortal. Cancer Res. 83, 3861–3867. https://doi.org/10.1158/0008-5472.CAN-23-0816.

Byers, L.A., Diao, L., Wang, J., Saintigny, P., Girard, L., Peyton, M., Shen, L., Fan, Y., Giri, U., Tumula, P.K., Nilsson, M.B., Gudikote, J., Tran, H., Cardnell, R.J.G., Bearss, D.J., Warner, S.L., Foulks, J.M., Kanner, S.B., Gandhi, V., Krett, N., Rosen, S. T., Kim, E.S., Herbst, R.S., Blumenschein, G.R., Lee, J.J., Lippman, S.M., Ang, K.K., Mills, G.B., Hong, W.K., Weinstein, J.N., Wistuba, I.I., Coombes, K.R., Minna, J.D., Heymach, J.V., 2013. An epithelial-mesenchymal transition gene signature predicts resistance to EGFR and PI3K inhibitors and identifies Axl as a therapeutic target for overcoming EGFR inhibitor resistance. Clin. Cancer Res. Off. J. Am. Assoc. Cancer Res. 19, 279–290. https://doi.org/10.1158/1078-0432.CCR-12-1558.

Catasus, L., Gallardo, A., Llorente-Cortes, V., Escuin, D., Muñoz, J., Tibau, A., Peiro, G., Barnadas, A., Lerma, E., 2011a. Low-density lipoprotein receptor-related protein 1 is associated with proliferation and invasiveness in Her-2/neu and triple-negative breast carcinomas. Hum. Pathol. 42, 1581–1588. https://doi.org/10.1016/j.humpath.2011.01.011.

Catasús, L., Llorente-Cortés, V., Cuatrecasas, M., Pons, C., Espinosa, I., Prat, J., 2011b. Low-density lipoprotein receptor-related protein 1 (LRP-1) is associated with highgrade, advanced stage and p53 and p16 alterations in endometrial carcinomas. Histopathology 59, 567–571. https://doi.org/10.1111/j.1365-2559.2011.03942.x.

Cerami, E., Gao, J., Dogrusoz, U., Gross, B.E., Sumer, S.O., Aksoy, B.A., Jacobsen, A., Byrne, C.J., Heuer, M.L., Larsson, E., Antipin, Y., Reva, B., Goldberg, A.P., Sander, C., Schultz, N., 2012. The cBio cancer genomics portal: an open platform for exploring multidimensional cancer genomics data. Cancer Discov. 2, 401–404. https://doi.org/10.1158/2159-8290.CD-12-0095.

Chae, Y.K., Chang, S., Ko, T., Anker, J., Agte, S., Iams, W., Choi, W.M., Lee, K., Cruz, M., 2018. Epithelial-mesenchymal transition (EMT) signature is inversely associated with T-cell infiltration in non-small cell lung cancer (NSCLC). Sci. Rep. 8, 2918. https://doi.org/10.1038/s41598-018-21061-1.

Chang, C., Tang, X., Mosallaei, D., Chen, M., Woodley, D.T., Schönthal, A.H., Li, W., 2022. LRP-1 receptor combines EGFR signalling and eHsp90α autocrine to support constitutive breast cancer cell motility in absence of blood supply. Sci. Rep. 12, 12006. https://doi.org/10.1038/s41598-022-16161-y.

Chen, J., Yang, H., Teo, A.S.M., Amer, L.B., Sherbaf, F.G., Tan, C.Q., Alvarez, J.J.S., Lu, B., Lim, J.Q., Takano, A., Nahar, R., Lee, Y.Y., Phua, C.Z.J., Chua, K.P., Suteja, L., Chen, P.J., Chang, M.M., Koh, T.P.T., Ong, B.-H., Anantham, D., Hsu, A.A.L., Gogna, A., Too, C.W., Aung, Z.W., Lee, Y.F., Wang, L., Lim, T.K.H., Wilm, A., Choi, P. S., Ng, P.Y., Toh, C.K., Lim, W.-T., Ma, S., Lim, B., Liu, J., Tam, W.L., Skanderup, A. J., Yeong, J.P.S., Tan, E.-H., Creasy, C.L., Tan, D.S.W., Hillmer, A.M., Zhai, W., 2020. Genomic landscape of lung adenocarcinoma in East Asians. Nat. Genet. 52, 177–186. https://doi.org/10.1038/s41588-019-0569-6.

Cruz Da Silva, E., Choulier, L., Thevenard-Devy, J., Schneider, C., Carl, P., Rondé, P., Dedieu, S., Lehmann, M., 2021. Role of endocytosis proteins in gefitinib-mediated EGFR internalisation in glioma cells. Cells 10, 3258. https://doi.org/10.3390/cells10113258.

Da Silva, J., Jouida, A., Ancel, J., Dalstein, V., Routhier, J., Delepine, G., Cutrona, J., Jonquet, A., Dewolf, M., Birembaut, P., Deslée, G., Polette, M., Nawrocki-Raby, B., 2020. FHITlow/pHER2high signature in non-small cell lung cancer is predictive of anti-HER2 molecule efficacy. J. Pathol. 251, 187–199. https://doi.org/10.1002/path.5439.

Dong, H., Zou, M., Bhatia, A., Jayaprakash, P., Hofman, F., Ying, Q., Chen, M., Woodley, D.T., Li, W., 2016. Breast cancer MDA-MB-231 cells use secreted heat shock protein-90alpha (Hsp90α) to survive a hostile hypoxic environment. Sci. Rep. 6, 20605. https://doi.org/10.1038/srep20605.

Fayard, B., Bianchi, F., Dey, J., Moreno, E., Djaffer, S., Hynes, N.E., Monard, D., 2009. The serine protease inhibitor protease nexin-1 controls mammary cancer metastasis through LRP-1-mediated MMP-9 expression. Cancer Res. 69, 5690–5698. https://doi.org/10.1158/0008-5472.CAN-08-4573.

Feng, C., Ding, G., Ding, Q., Wen, H., 2018. Overexpression of low density lipoprotein receptor-related protein 1 (LRP1) is associated with worsened prognosis and decreased cancer immunity in clear-cell renal cell carcinoma. Biochem. Biophys. Res. Commun. 503, 1537–1543. https://doi.org/10.1016/j.bbrc.2018.07.076.

Gao, J., Aksoy, B.A., Dogrusoz, U., Dresdner, G., Gross, B., Sumer, S.O., Sun, Y., Jacobsen, A., Sinha, R., Larsson, E., Cerami, E., Sander, C., Schultz, N., 2013. Integrative analysis of complex cancer genomics and clinical profiles using the cBioPortal. Sci. Signal. 6. https://doi.org/10.1126/scisignal.2004088.

Ghandi, M., Huang, F.W., Jané-Valbuena, J., Kryukov, G.V., Lo, C.C., McDonald, E.R., Barretina, J., Gelfand, E.T., Bielski, C.M., Li, H., Hu, K., Andreev-Drakhlin, A.Y., Kim, J., Hess, J.M., Haas, B.J., Aguet, F., Weir, B.A., Rothberg, M.V., Paolella, B.R., Lawrence, M.S., Akbani, R., Lu, Y., Tiv, H.L., Gokhale, P.C., de Weck, A., Mansour, A. A., Oh, C., Shih, J., Hadi, K., Rosen, Y., Bistline, J., Venkatesan, K., Reddy, A., Sonkin, D., Liu, M., Lehar, J., Korn, J.M., Porter, D.A., Jones, M.D., Golji, J., Caponigro, G., Taylor, J.E., Dunning, C.M., Creech, A.L., Warren, A.C., McFarland, J. M., Zamanighomi, M., Kauffmann, A., Stransky, N., Imielinski, M., Maruvka, Y.E., Cherniack, A.D., Tsherniak, A., Vazquez, F., Jaffe, J.D., Lane, A.A., Weinstock, D.M., Johannessen, C.M., Morrissey, M.P., Stegmeier, F., Schlegel, R., Hahn, W.C., Getz, G., Mills, G.B., Boehm, J.S., Golub, T.R., Garraway, L.A., Sellers, W.R., 2019. Next-generation characterization of the cancer cell line encyclopedia. Nature 569, 503–508. https://doi.org/10.1038/s41586-019-1186-3.

Herz, J., Hamann, U., Rogne, S., Myklebost, O., Gausepohl, H., Stanley, K.K., 1988. Surface location and high affinity for calcium of a 500-kd liver membrane protein closely related to the LDL-receptor suggest a physiological role as lipoprotein receptor. EMBO J. 7, 4119–4127. https://doi.org/10.1002/j.1460-2075.1988.tb03306.x.

Huang, X.-Y., Shi, G.-M., Devbhandari, R.P., Ke, A.-W., Wang, Y., Wang, X.-Y., Wang, Z., Shi, Y.-H., Xiao, Y.-S., Ding, Z.-B., Dai, Z., Xu, Y., Jia, W.-P., Tang, Z.-Y., Fan, J., Zhou, J., 2012. Low level of low-density lipoprotein receptor-related protein 1 predicts an unfavorable prognosis of hepatocellular carcinoma after curative resection. PLOS One 7, e32775. https://doi.org/10.1371/journal.pone.0032775.

Joannes, A., Bonnomet, A., Bindels, S., Polette, M., Gilles, C., Burlet, H., Cutrona, J., Zahm, J.-M., Birembaut, P., Nawrocki-Raby, B., 2010. Fhit regulates invasion of lung tumor cells. Oncogene 29, 1203–1213. https://doi.org/10.1038/onc.2009.418.

Joannes, A., Grelet, S., Duca, L., Gilles, C., Kileztky, C., Dalstein, V., Birembaut, P., Polette, M., Nawrocki-Raby, B., 2014. Fhit regulates EMT targets through an EGFR/Src/ERK/Slug signaling axis in human bronchial cells. Mol. Cancer Res. 12, 775–783. https://doi.org/10.1158/1541-7786.MCR-13-0386-T.

Langlois, B., Perrot, G., Schneider, C., Henriet, P., Emonard, H., Martiny, L., Dedieu, S., 2010. LRP-1 promotes cancer cell invasion by supporting ERK and inhibiting JNK signaling pathways. PLOS One 5, e11584. https://doi.org/10.1371/journal.pone.0011584.

Le, C.C., Bennasroune, A., Collin, G., Hachet, C., Lehrter, V., Rioult, D., Dedieu, S., Morjani, H., Appert-Collin, A., 2020. LRP-1 promotes colon cancer cell proliferation in 3D collagen matrices by mediating DDR1 endocytosis. Front. Cell Dev. Biol. 8, 412. https://doi.org/10.3389/fcell.2020.00412.

Loeffler, E., Ancel, J., Dalstein, V., Deslée, G., Polette, M., Nawrocki-Raby, B., 2023. HER2 alterations in non-small cell lung cancer: biologico-clinical consequences and interest in therapeutic strategies. Life 14, 64. https://doi.org/10.3390/life14010064.

Mak, M.P., Tong, P., Diao, L., Cardnell, R.J., Gibbons, D.L., William, W.N., Skoulidis, F., Parra, E.R., Rodriguez-Canales, J., Wistuba, I.I., Heymach, J.V., Weinstein, J.N., Coombes, K.R., Wang, J., Byers, L.A., 2016. A patient-derived, pan-cancer EMT signature identifies global molecular alterations and immune target enrichment following epithelial-to-mesenchymal transition. Clin. Cancer Res. Off. J. Am. Assoc. Cancer Res. 22, 609–620. https://doi.org/10.1158/1078-0432.CCR-15-0876.

Meng, H., Chen, G., Zhang, X., Wang, Z., Thomas, D.G., Giordano, T.J., Beer, D.G., Wang, M.M., 2011. Stromal LRP1 in lung adenocarcinoma predicts clinical outcome. Clin. Cancer Res. Off. J. Am. Assoc. Cancer Res. 17, 2426–2433. https://doi.org/10.1158/1078-0432.CCR-10-2385.

Niu, Z., Jiang, D., Shen, J., Liu, W., Tan, X., Cao, G., 2023. Potential role of the fragile histidine triad in cancer evo-dev. Cancers 15, 1144. https://doi.org/10.3390/cancers15041144.

Ohta, M., Inoue, H., Cotticelli, M.G., Kastury, K., Baffa, R., Palazzo, J., Siprashvili, Z., Mori, M., McCue, P., Druck, T., Croce, C.M., Huebner, K., 1996. The FHIT gene, spanning the chromosome 3p14.2 fragile site and renal carcinoma-associated t(3;8) breakpoint, is abnormal in digestive tract cancers. Cell 84, 587–597. https://doi.org/10.1016/s0092-8674(00)81034-x.

Pekarsky, Y., Zanesi, N., Palamarchuk, A., Huebner, K., Croce, C.M., 2002. FHIT: from gene discovery to cancer treatment and prevention. Lancet Oncol. 3, 748–754. https://doi.org/10.1016/S1470-2045(02)00931-2.

Roz, L., Gramegna, M., Ishii, H., Croce, C.M., Sozzi, G., 2002. Restoration of fragile histidine triad (FHIT) expression induces apoptosis and suppresses tumorigenicity in lung and cervical cancer cell lines. Proc. Natl. Acad. Sci. USA 99, 3615–3620. https://doi.org/10.1073/pnas.062030799.

Sahu, D., Zhao, Z., Tsen, F., Cheng, C.-F., Park, R., Situ, A.J., Dai, J., Eginli, A., Shams, S., Chen, M., Ulmer, T.S., Conti, P., Woodley, D.T., Li, W., 2012. A potentially common peptide target in secreted heat shock protein-90α for hypoxia-inducible factor-1α-positive tumors. Mol. Biol. Cell 23, 602–613. https://doi.org/10.1091/mbc.E11-06-0575.

Salama, Y., Lin, S.-Y., Dhahri, D., Hattori, K., Heissig, B., 2019. The fibrinolytic factor tPA drives LRP1-mediated melanoma growth and metastasis. FASEB J. Off. Publ. Fed. Am. Soc. Exp. Biol. 33, 3465–3480. https://doi.org/10.1096/fj.201801339RRR.

Saldivar, J.C., Miuma, S., Bene, J., Hosseini, S.A., Shibata, H., Sun, J., Wheeler, L.J., Mathews, C.K., Huebner, K., 2012. Initiation of genome instability and preneoplastic processes through loss of Fhit expression. PLOS Genet. 8, e1003077. https://doi.org/10.1371/journal.pgen.1003077.

Sizova, O., John, L.S., Ma, Q., Molldrem, J.J., 2023. Multi-faceted role of LRP1 in the immune system. Front. Immunol. 14, 1166189. https://doi.org/10.3389/fimmu.2023.1166189.

Song, H., Li, Y., Lee, J., Schwartz, A.L., Bu, G., 2009. Low-density lipoprotein receptor-related protein 1 promotes cancer cell migration and invasion by inducing the expression of matrix metalloproteinases 2 and 9. Cancer Res. 69, 879–886. https://doi.org/10.1158/0008-5472.CAN-08-3379.

Sozzi, G., Veronese, M.L., Negrini, M., Baffa, R., Cotticelli, M.G., Inoue, H., Tornielli, S., Pilotti, S., De Gregorio, L., Pastorino, U., Pierotti, M.A., Ohta, M., Huebner, K., Croce, C.M., 1996. The FHIT gene 3p14.2 is abnormal in lung cancer. Cell 85, 17–26. https://doi.org/10.1016/s0092-8674(00)81078-8.

Strickland, D.K., Ashcom, J.D., Williams, S., Burgess, W.H., Migliorini, M., Argraves, W. S., 1990. Sequence identity between the alpha 2-macroglobulin receptor and low density lipoprotein receptor-related protein suggests that this molecule is a multifunctional receptor. J. Biol. Chem. 265, 17401–17404.

Suh, S.-S., Yoo, J.Y., Cui, R., Kaur, B., Huebner, K., Lee, T.-K., Aqeilan, R.I., Croce, C.M., 2014. FHIT suppresses epithelial-mesenchymal transition (EMT) and metastasis in lung cancer through modulation of microRNAs. PLOS Genet. 10, e1004652. https://doi.org/10.1371/journal.pgen.1004652.

Sung, H., Ferlay, J., Siegel, R.L., Laversanne, M., Soerjomataram, I., Jemal, A., Bray, F., 2021. Global cancer statistics 2020: GLOBOCAN estimates of incidence and mortality worldwide for 36 cancers in 185 countries. Cancer J. Clin. 71, 209–249. https://doi.org/10.3322/caac.21660.

Thai, A.A., Solomon, B.J., Sequist, L.V., Gainor, J.F., Heist, R.S., 2021. Lung cancer. Lancet 398, 535–554. https://doi.org/10.1016/S0140-6736(21)00312-3.

Tian, Y., Wang, C., Chen, S., Liu, J., Fu, Y., Luo, Y., 2019. Extracellular Hsp90α and clusterin synergistically promote breast cancer epithelial-to-mesenchymal transition and metastasis via LRP1. J. Cell Sci. 132, jcs228213. https://doi.org/10.1242/jcs.228213.

Van Gool, B., Dedieu, S., Emonard, H., Roebroek, A.J.M., 2015. The matricellular receptor LRP1 forms an interface for signaling and endocytosis in modulation of the extracellular tumor environment. Front. Pharmacol. 6, 271. https://doi.org/10.3389/fphar.2015.00271.

de Vries, T.J., Verheijen, J.H., de Bart, A.C., Weidle, U.H., Ruiter, D.J., van Muijen, G.N., 1996. Decreased expression of both the low-density lipoprotein receptor-related protein/alpha(2)-macroglobulin receptor and its receptor-associated protein in late stages of cutaneous melanocytic tumor progression. Cancer Res. 56, 1432–1439.

Xue, N., Du, T., Lai, F., Jin, J., Ji, M., Chen, X., 2022. Secreted HSP90α-LRP1 signaling promotes tumor metastasis and chemoresistance in pancreatic cancer. Int. J. Mol. Sci. 23, 5532. https://doi.org/10.3390/ijms23105532.